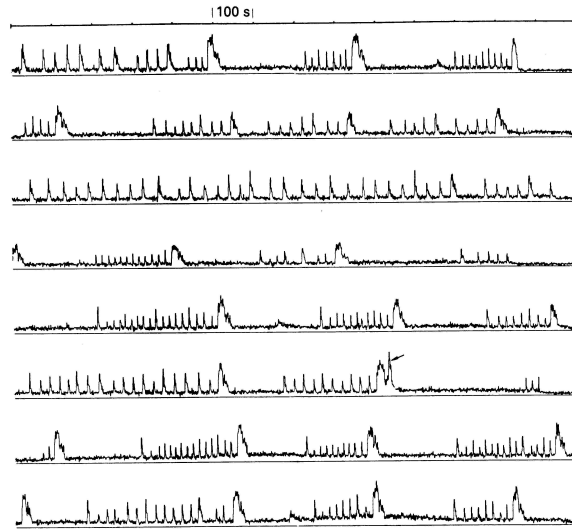




24-minute snapshots from 8 orbits on March 2/3, 1976

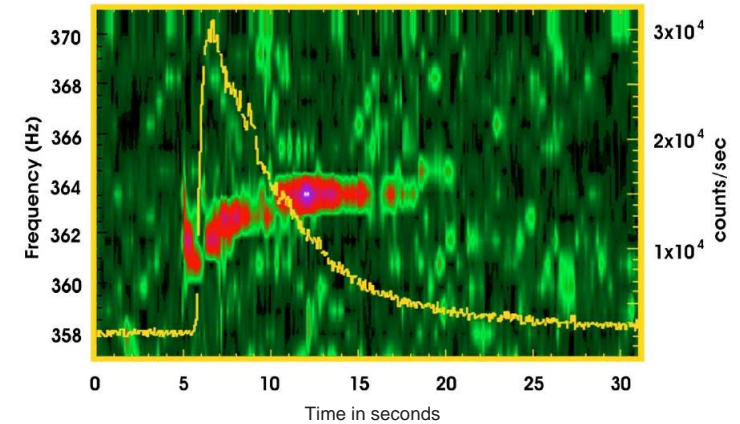


(Joss & Rappaport, 1984, Fig. 18)

Bursting of the "Rapid Burster" MXB1730-335: Type I and Type II bursts.

Type II bursts: magnetospheric gate model: B -field blocks accretion until $P_{\text{gas}} > P_{\text{mag}} \Rightarrow \text{BOOM}$.

Burst oscillations

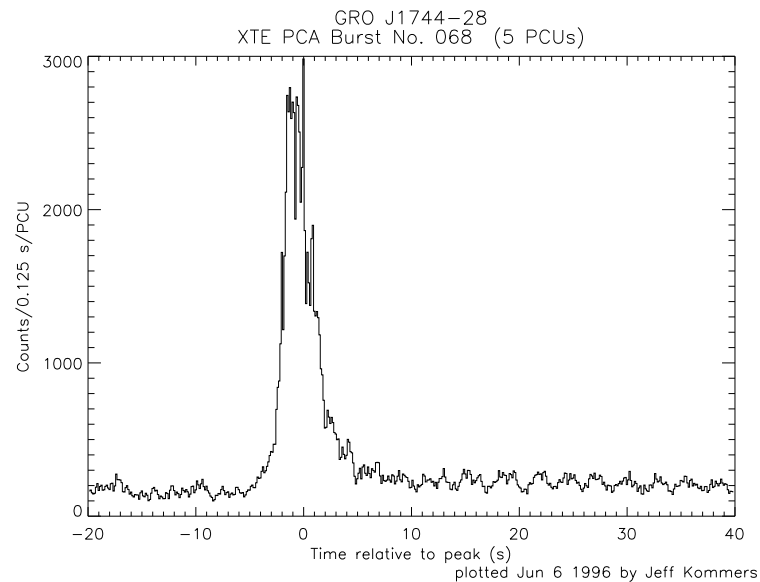


(after Galloway et al., 2006, Fig. 3; colors: power spectrum)

Burst oscillation: strong, coherent oscillation in decay of burst with long term stability. Asymptotic frequency \sim agrees with pulsar rotational frequency

Bursting Pulsar

2



(Bursting Pulsar; Kommers, 1996, priv. comm.)

Before 1995 December 2: X-ray bursts and pulsations cannot occur in the same object.

Then: GRO J1744-28 the bursting pulsar. Pulsations with 2 Hz and type II bursts. *Burst rate*: $\sim 20 \text{ h}^{-1}$, then decreasing to 1 h^{-1} . Orbit $\sim 2 \text{ d}$. Source temporarily brightest X-ray source in the sky (several Crab).

Timing

To describe the variability of an evenly spaced time series $x_k = x(t_k = k\Delta t)$ we use the Discrete Fourier Transform $X_j = X(f_j = j/N\Delta t)$

$$X_j = \sum_{k=0}^{N-1} x_k \exp(2\pi i j k / N) \quad , \text{ for } j = 1 \dots N/2 \quad (6.11)$$

Remember: $\exp(i\phi) = \cos \phi + i \sin \phi$ The amount of variability at a frequency f_j is then characterized by the Power Spectral Density,

$$\text{PSD}_j = A X_j^* X_j \quad (6.12)$$

where A is a normalization constant.

To reduce scatter, one often averages the power spectra of several data segments.

The PSD describes the contribution of a given frequency to the total variance of the lightcurve (power).

One often uses the Miyamoto normalization where

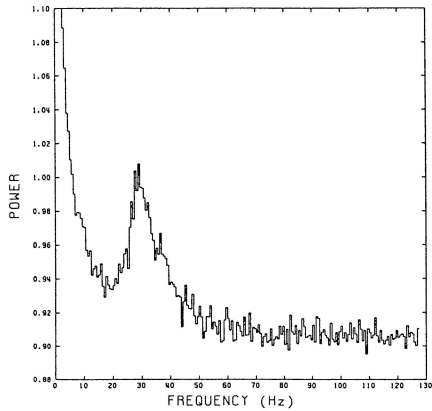
$$A_{\text{Miyamoto}} \iff (\text{rms}/\langle \text{rate} \rangle)^2 \text{ Hz}^{-1} \quad (6.13)$$

LMXB Timing Properties

1



EXOSAT: The QPO Era, I



1985, IAUC 4043:
 “EXOSAT observations of the bright galactic-bulge source GX 5–1 made during 1984 Sept. 18.46–18.83 UT with a time resolution of 0.25 ms show the presence of quasiperiodic oscillations of the 1–10 keV flux with a typical period between 25 and 50 ms [20–40 Hz].”

“Since this is the discovery of a new phenomenon, we urge observers to search for similar X-ray behavior in other sources . . .”

van der Klis, Jansen, van Paradijs, Lewin, van den Heuvel, Trümper, Szatjno

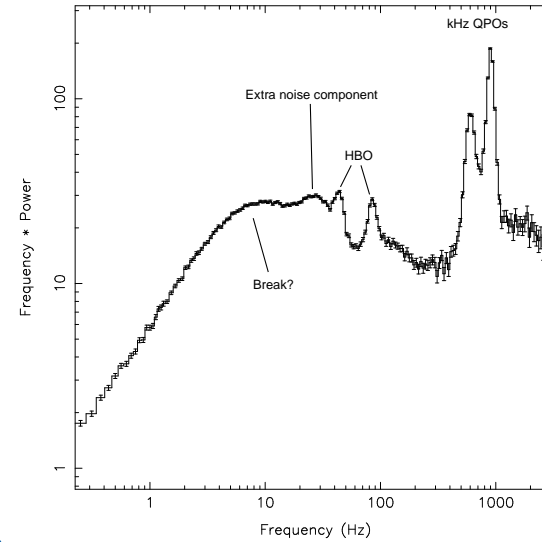
EXOSAT ME: 1–20 keV, $A_{\text{eff}} = 1600 \text{ cm}^2$, $\Delta t \sim 0.25 \text{ ms}$

LMXB Timing Properties

2



RXTE: The KiloHertz QPO Era, I



“The kHz QPO are the most important scientific result to date of RXTE”.

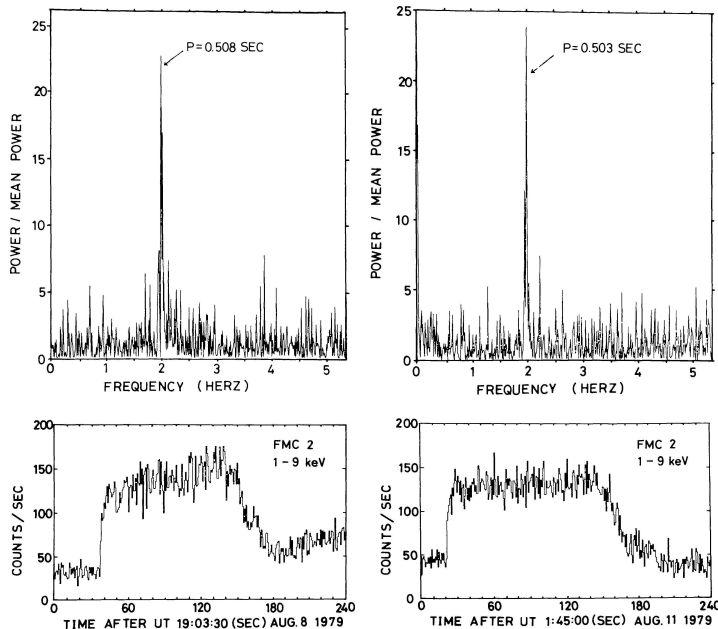
(<http://heasarc.gsfc.nasa.gov/docs/xte/Great>)

RXTE PCA: 2–25 keV, $A_{\text{eff}} = 5000 \text{ cm}^2$, $\Delta t = 1 \mu\text{s}$

Sco X-1; *van der Klis et al., 1996, IAUC 6319, Wijnands & van der Klis (1999)*

LMXB Timing Properties

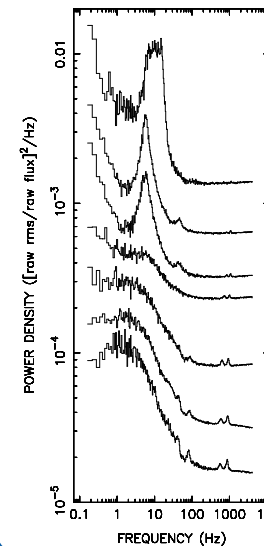
4



(QPOs during type II bursts of the rapid burster; *Lewin, van Paradijs & van der Klis, 1988, Fig. 1.3*)



RXTE: The KiloHertz QPO Era, II



- always have 3 characteristic frequencies:
 - “Low Frequency QPOs” (ν_{LF}): 0.1–100 Hz, many types
 - “kHz Twin Peaks” (ν_1, ν_2): 200–1400 Hz
- “real” kHz QPOs only for neutron star binaries, mostly persistent LMXBs, $\gtrsim 20$ kHz QPO sources are known, mostly showing double peaks

The kHz QPO strength is flux dependent.

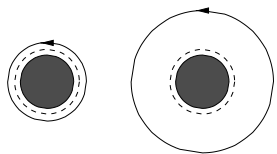
(*Wijnands & van der Klis, 1999*)

LMXB Timing Properties

5



Origin of QPOs



1200 Hz

500 Hz

kHz QPOs occur on timescales close to the innermost stable circular orbit:

The Keplerian orbit frequency is:

$$\nu_{\text{orb}} = \left(\frac{GM}{4\pi^2 R_{\text{orb}}^3} \right)^{1/2} \approx 1200 \text{ Hz} \left(\frac{R_{\text{orb}}}{15 \text{ km}} \right)^{-3/2} m_{1.4}^{1/2} \quad (6.14)$$

The edge of the accretion disk is at the innermost stable circular orbit (ISCO), Schwarzschild geometry:

$$R_{\text{ISCO}} = \frac{6GM}{c^2} \sim 12.5 M_{1.4} \text{ km} \quad (6.15)$$

and therefore the maximum stable frequency in an accretion disk is

$$\nu_{\text{ISCO}} \sim \frac{1580 \text{ Hz}}{M_{1.4}} \quad (6.16)$$

Corrections due to the spin of the central object can amount to several 10%



Beat Frequency Model, I

“beat”: resonance between some preferred Keplerian orbit & spin frequency

Magnetospheric BFM:

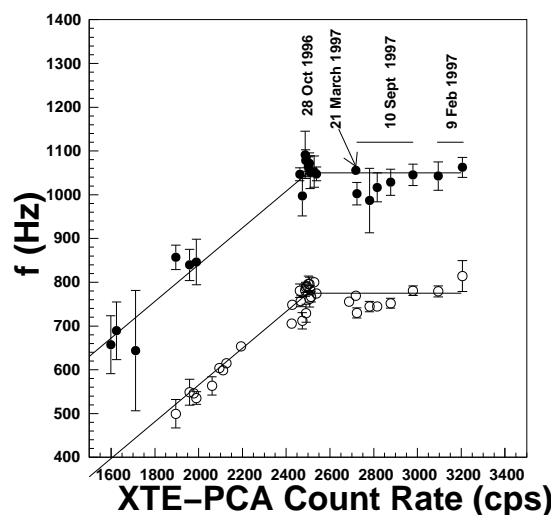
- preferred radius = Alfvén radius
 - orbiting clump ($\nu_{\text{Alfvén}}$) modulated by B -field (ν_{spin})
- ⇒ can explain LF QPOs, 5–50 Hz

Sonic Point BFM:

- preferred radius = where radial inflow velocity becomes supersonic, near ISCO
- orbiting clump ($\nu_{\text{sonic}} > \nu_{\text{spin}}$) causes bright footpoint near surface, **footpoint: upper kHz QPO, $\nu_2 = \nu_{\text{sonic}}$**
- clumps are irradiated with ν_{spin} ⇒ footpoint emission is modulated with beat between ν_{sonic} and ν_{spin} , **footpoint modulation: lower kHz QPO, $\nu_1 = \nu_{\text{beat}}$**



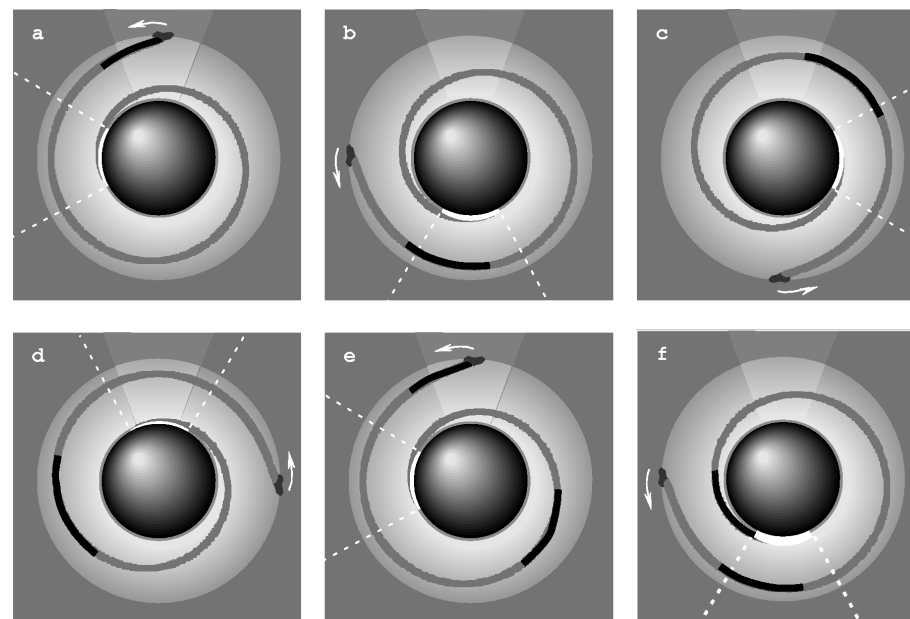
Origin of QPOs



The frequencies of kHz QPOs usually increase with X-ray flux (“parallel-lines phenomenon”), and can saturate at a maximum frequency.

⇒ Models need to explain ν_{LF} , ν_1 , and ν_2 .

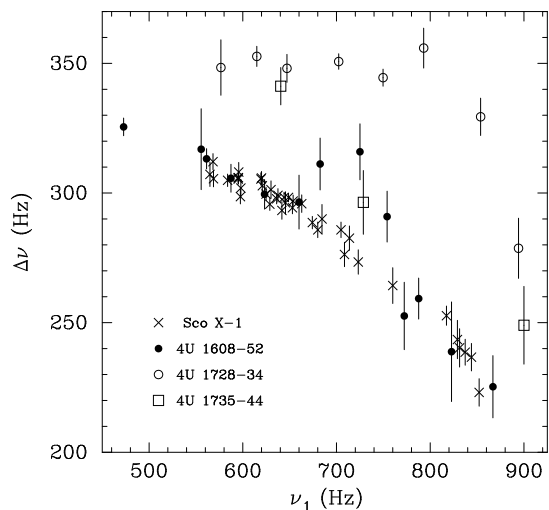
(4U 1820–30; Zhang et al., 1998)



(Miller, Lamb & Psaltis, 1998)



Beat Frequency Model, III



There is a varying frequency separation between the kHz QPOs of different sources
 \Rightarrow problem for the beat frequency model?

(van der Klis, 2000)



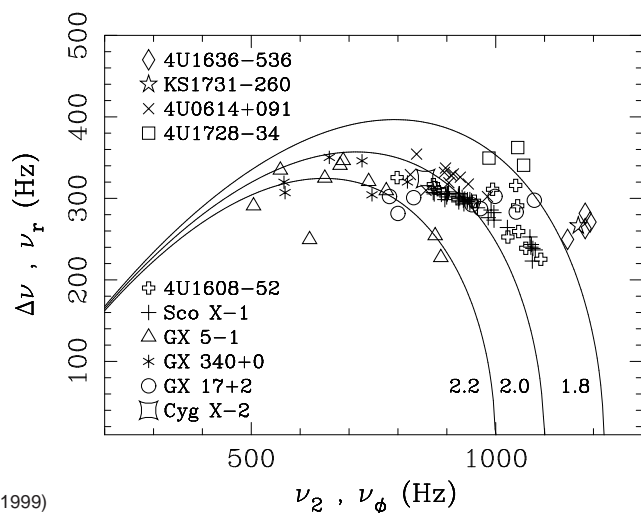
Beat Frequency Model, V

Properties & problems of the sonic point beat frequency model:

- needs surface
 \Rightarrow not valid for BHC sources
- Keplerian motion inside $r_{\text{Alfén}}$
- r_{sonic} depends on \dot{M}
 \Rightarrow varying ν_2 can be explained
- $\Delta\nu = \nu_2 - \nu_1$, constant, can be $< \nu_{\text{spin}}$
 \Rightarrow varying $\Delta\nu$ cannot easily be explained
- predicts additional frequencies (differing from precession model)



Beat Frequency Model, IV



(Stella & Vietri, 1999)

The frequency separation of the QPOs varies differently in different sources.



Relativistic Precession Model, I

General Relativity: free-particle orbits show characteristic frequencies

Idea of the model:

- disk is disrupted near ISCO, forming blobs
- blob orbits are inclined and eccentric

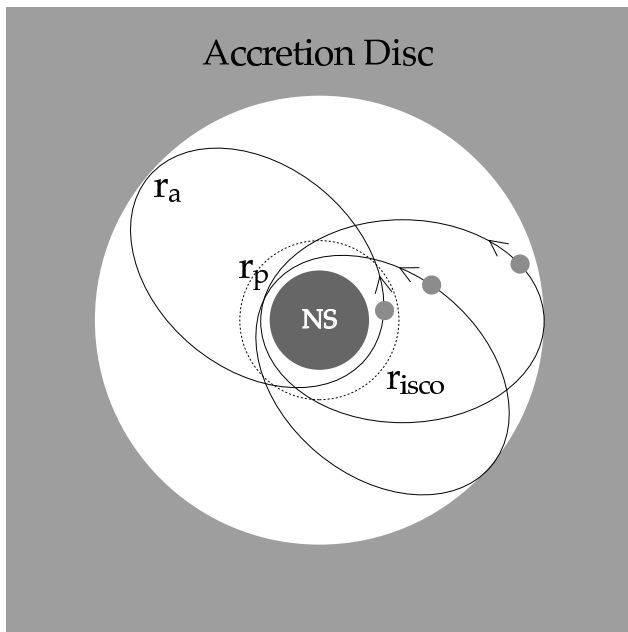
Characteristic frequencies:

- orbit frequency: upper kHz QPO, ν_2
- periastron precession: lower kHz QPO, ν_1
- relativistic frame dragging \rightarrow "wobble of the orbital plane":
 nodal precession (Lense-Thirring)

$$\nu_{\text{LF}} = 2 \times \nu_{\text{nod}}$$

$$\nu_{\text{nod}} = 8\pi^2 I \nu_2^2 \nu_{\text{spin}} / c^2 M, \quad \text{where } I: \text{ moment of inertia}$$

see, e.g., Stella & Vietri (1998)



(Marković & Lamb, 1998, see also Marković & Lamb, 2000, astro-ph/0009169)



Model Summary

Promises:

- constrain M and R (via kHz QPOs)
 \implies constrain Equation of State for neutron stars
- constrain spin
 (“holy grail”, LMXB/ms radio pulsar evolution?!)
- constrain B-field (via LF QPOs)
- observe GR effects

Difficulties:

- observations (varying $\Delta\nu_{\text{kHz}}$, ν -correlations)
 triggered evolution of many different models (> 12)
- no individual model does address all issues
 (i.e. generation of flux modulation, ...)
- models predict different ν_{spin} and M , e.g.,
 BFM: $\nu_{\text{spin}} = 250\text{--}350$ Hz
 RPM: $\nu_{\text{spin}} = 300\text{--}900$ Hz
- what about “surface models”? \iff big question: do BHCs show the same behavior as neutron star XRBs?

Models for QPOs



Relativistic Precession Model, III

Properties & problems of the RPM:

- does not need surface
 \implies also valid for BHC sources
- can explain $\Delta\nu$ (more or less)
- how to disrupt the disk?
 how to create compact clumps?
 how to maintain tilted orbits?
- how to create the flux modulations?
- other frequencies could be more important

Models for QPOs

Church, M. J., 2004, in Revista Mexicana de Astronomia y Astrofisica Conference Series, ed. G. Tovmassian, E. Sion, Vol. 20, 140

Church, M. J., & Balucinska-Church, M., 1995, A&A, 300, 441

Cumming, A., 2004, Nucl. Phys. B Proc. Suppl., 132, 435

Cumming, A., & Bildsten, L., 2001, ApJ, 559, L127

Galloway, D. K., Muno, M. P., Hartman, J. M., Savov, P., Psaltis, D., & Chakrabarty, D., 2006, ApJS, submitted (astro-ph/0608259)

Grimm, H.-J., Gilfanov, M., & Sunyaev, R., 2003, Ch. J. Astron. Astrophys. Suppl., 3, 257

Hansen, C. J., & van Horn, H. M., 1975, ApJ, 195, 735

Hasinger, G., & van der Klis, M., 1989, A&A, 225, 79

Jonker, P. G., et al., 2000, ApJ, 537, 374

Joss, P. C., & Rappaport, S. A., 1984, Ann. Rev. Astron. Astrophys., 22, 537

Kuulkers, E., 2004, Nucl. Phys. B Proc. Suppl., 132, 466

Lamb, D. Q., & Lamb, F. K., 1978, ApJ, 220, 291

Lewin, W. H. G., van Paradijs, J., & Taam, R. E., 1993, Space Sci. Rev., 62, 223

Lewin, W. H. G., van Paradijs, J., & van der Klis, M., 1988, Space Sci. Rev., 46, 273

Marković, D., & Lamb, F. K., 1998, ApJ, 507, 316

Méndez, M., van der Klis, M., Ford, E. C., Wijnands, R., & van Paradijs, J., 1999, ApJ, 511, L49

Miller, M. C., Lamb, F. K., & Psaltis, D., 1998, ApJ, 508, 791

Mitsuda, K., Inoue, H., Nakamura, N., & Tanaka, Y., 1989, PASJ, 41, 97

Schatz, H., & Rehm, K. E., 2006, Nucl. Phys. A, 777, 601

Stella, L., & Vietri, M., 1998, ApJ, 492, L49

Stella, L., & Vietri, M., 1999, Phys. Rev. Lett., 82, 17

Strohmayer, T., & Bildsten, L., 2006, in *Compact stellar X-ray sources*, ed. W. Lewin, M. van der Klis, (Cambridge: Cambridge Univ. Press), 113-156

Swank, J. H., Becker, R. H., Boldt, E. A., Holt, S. S., Pravdo, S. H., & Serlemitsos, P. J., 1977, *ApJ*, 212, L73

Taam, R. E., & Picklum, R. E., 1979, *ApJ*, 233, 327

van der Klis, M., 1989, *Ann. Rev. Astron. Astrophys.*, 27, 517

van der Klis, M., 2000, *Ann. Rev. Astron. Astrophys.*, 38, 717

van Straaten, S., van der Klis, M., & Méndez, M., 2003, *ApJ*, 596, 1155

White, N. E., Stella, L., & Parmar, A. N., 1988, *ApJ*, 324, 363

Wijnands, R., & van der Klis, M., 1999, *ApJ*, 514, 939

Zhang, W., Smale, A. P., Strohmayer, T. E., & Swank, J. H., 1998, *ApJ*, 500, L171

Zingale, M., et al., 2001, *ApJS*, 133, 195